Tunable wavelength terahertz polarization converter based on quartz waveplates

A. K. Kaveev,[1,*] G. I. Kropotov,[1] D. I. Tsypishka,[1] I. A. Tzibizov,[1] I. A. Vinerov,[1] and E. G. Kaveeva[2]

[1]TYDEX LLC, 194292 St. Petersburg, Russia

[2]St. Petersburg State Polytechnic University, 195251 St. Petersburg, Russia

*Corresponding author: andreykaveev@tydex.ru

Received 1 April 2014; revised 8 July 2014; accepted 17 July 2014;
posted 18 July 2014 (Doc. ID 209267); published 14 August 2014

We present the results of calculation and experimental testing of the tunable wavelength terahertz polarization converter represented by a set of plane-parallel birefringent plates with an in-plane birefringence axis. An experimental device has been produced and tested. The calculations show that the effect of interference between the interfaces, including air gaps, may be neglected. The considered device may be used as a simple narrow achromatic waveplate, or a Solc band pass filter for the specified wavelength. © 2014 Optical Society of America

OCIS codes: (040.2235) Far infrared or terahertz; (230.5440) Polarization-selective devices.
http://dx.doi.org/10.1364/AO.53.005410

1. Introduction

The terahertz (THz) frequency range (300 GHz–10 THz) is a quite significant portion of the electromagnetic spectrum lying between the microwave and infrared ranges. Unlike the latter, the THz range was virtually unexplored until recently, due to the absence of both powerful THz sources and detectors operating in this wavelength range. Promising applications of THz radiation include ultrafast secure data exchange, internal and external communications in integrated circuits, spectroscopy (namely, determining the chemical composition of complex substances, due to the fact that many vibrational and rotational levels of large organic molecules occur in the THz range), security and alarm systems, and explosive, weapon, and drug detection [1–5]. Besides, THz radiation can be very promising in tomographic and medical applications [4,6].

Rapid progress in THz optoelectronics necessitates the development of optical component production for the THz spectral range as demanded by the specifics of the instruments operating in the aforementioned range. The material traditionally used for THz instrumentation is crystalline quartz. Its transmission spectrum in the spectral range of interest is shown in Fig. 1.

There are many other traditional materials for THz optics, for example, PE, PP, Teflon, fused silica, and high-resistivity silicon. Besides, crystalline quartz is a birefringent material [7]; this fact makes possible its use in THz optics to create polarization-converting components. In this paper we present theoretical calculations and modeling as well as experimental studies of several such components based on crystalline quartz. It should be noted that any other birefringent material transparent in the THz range may be used instead of quartz, such as sapphire or boron nitride. The birefringence axis must lie in the plane of the plates, which constitutes a technological limitation in the latter case.

2. Results

In this work, we have modeled, produced, and tested the tunable wavelength THz polarization converter

1559-128X/14/245410-06$15.00/0

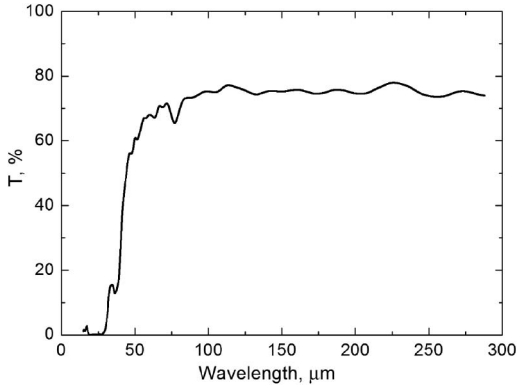

Fig. 1. Transmission spectrum of crystalline quartz, thickness 0.4 mm, x-oriented.

(TWPC). This object consists of a set of parallel-plane birefringent plates made of the same material, which are transparent in the THz wavelength range with optical axes of birefringence lying in the plate plane. Unlike the monochromatic waveplate (WP), which provides necessary phase retardation for concrete wavelength, the tunable wavelength polarization converter provides the ability to tune the retardation in a wide wavelength range.

The paper [8] establishes that to achieve controlled adjustment of a retardation plate for a specific wavelength and arbitrary retardation, a set of three identical waveplates is sufficient, with the outermost plates having parallel birefringence axes. The angle between them and the optical axis of the middle plate must be calculated using a certain method. After that the construction is oriented with the special azimuthal angle relative to the azimuth of the electric field vector of the incident beam. This angle can be calculated in the same way as the angle between optical axes of the plates in the assembly. If the assembly allows one to adjust orientation angles (i.e., the plates are not in optical contact and not glued), the set may be fairly well adjusted for a series of arbitrary wavelengths and operate as a quarter-wave or half-wave plate. Rather than being achromatic or superachromatic, the composite retardation plates are controllable waveplates.

A. Calculation

There are several papers [9–14] related to the calculation methods of quartz and sapphire achromatic WPs. Some corrections were described in these basic methods for WP calculations. Namely, there were some modifications of methods that take into account the interference effect. The general novelty of the present work is an application and modification of the method to the calculation of the device based on three rotatable independent plates. Being based on the device, different polarization transformers may be obtained. The first is the TWPC; i.e., in Tydex LLC we have applied the methods for the real WP calculations. We have found that in the TWPC system the interference effect may be neglected in the case in which the system resolution is 2 cm^{-1} or more. Also we have carried out the measurements of TWPC, produced on the basis of the simulations. These experiments confirm the applicability of the methods described. Thus the production of the TWPC is achieved.

According to Jones formalism [15,16] the system of several retardation plates is optically equal to the system containing only two elements—a so-called "retarder" and "rotator."

The retarder provides the required phase shift (for example, π or $\pi/2$). The rotator turns the polarization plane at the angle ω. In the case of the symmetric system of waveplates (such as TWPC) there is no need for the rotator in the model. In this work we have calculated TWPCs for $\lambda/4$ and $\lambda/2$ cases in different THz ranges.

The TWPC is described by the simple Jones matrix 2×2:

$$\hat{J} = \prod_{i=1}^{3} \hat{J}_i,$$

$$\hat{J}_i = \begin{pmatrix} \cos\frac{\delta_i}{2} + j\cos(2\varphi_i)\sin\left(\frac{\delta_i}{2}\right) & j\sin(2\varphi_i)\sin\left(\frac{\delta_i}{2}\right) \\ j\sin(2\varphi_i)\sin\left(\frac{\delta_i}{2}\right) & \cos\frac{\delta_i}{2} - j\cos(2\varphi_i)\sin\left(\frac{\delta_i}{2}\right) \end{pmatrix}. \tag{1}$$

Here, $\delta_i = 2\pi(n_e - n_o)d_i/\lambda$, d_i is the width of the ith waveplate, and φ_i is the effective optical axis (EOA) angle of the plate relative to the chosen x axis (for example, the external polarizer axis).

The EOA angle relative to the x axis depends on Jones matrix components in this way:

$$\varphi = 0.5\left|\operatorname{arctg}\left(\frac{\mathrm{Im}(J_{12})\mathrm{Re}(J_{11}) + \mathrm{Re}(J_{12})\mathrm{Im}(J_{11})}{\mathrm{Im}(J_{11})\mathrm{Re}(J_{11}) - \mathrm{Re}(J_{12})\mathrm{Im}(J_{12})}\right)\right|, \tag{2}$$

and the retardation may be calculated with the formulas

$$\delta_0 = 2\,\mathrm{arctg}\sqrt{\frac{(\mathrm{Im}(J_{11}))^2 + (\mathrm{Im}(J_{12}))^2}{(\mathrm{Re}(J_{11}))^2 + (\mathrm{Re}(J_{12}))^2}}. \tag{3}$$

To evaluate the TWPC for specific retardation at specific wavelength, one must first calculate [8] the rotation angle α of the middle plate respective to the outer plates using the equation

$$\alpha = 0.5\,\arccos\left(\frac{\cos(\delta)\cos\left(\frac{\delta}{2}\right) - \cos\left(\frac{\delta_0}{2}\right)}{\sin(\delta)\sin\left(\frac{\delta}{2}\right)}\right), \tag{4}$$

where $\delta = 2\pi(n_o - n_e)d/\lambda$ (in our case $\delta = \delta_1 = \delta_2 = \delta_3$); δ_0 is the required retardation of the TWPC. Reasonable plate thickness should be selected to achieve TWPC operation in the required wavelength range. The TWPC's EOA rotation angle φ can be determined by substituting the calculated α value into the formulas (1) as the middle plate rotation

angle, i.e., $\varphi_2 = \alpha$, $\varphi_1 = \varphi_3 = 0$. After that, using the algorithm described in [17], interference corrections for these angles can be calculated.

In Fig. 2 the results of the retardation comparison for monochromatic WP and TWPC are shown. The cases of the half-wave plate [Fig. 2(a)] and quarter-wave plate [Fig. 2(b)] are described here. It can be seen that the same values of retardation for the TWPC and monochromatic WP are achieved.

Since the reconfigurable waveplate requires rotation of the middle plate relative to the outer ones, the design of the unit must provide an air gap between them. If one does not take into account the effect of the interference between the interfaces, there is no reason to take into account the interference in the gap. Generally, to evaluate such a system taking into account the interference, besides the matrices related to the waveplates, one needs to introduce two matrices to describe the air gap.

It should be noted that the necessity of the gap formation significantly complicates TWPC production, because it is desirable to provide the maximal parallelism of all the plates with the minimal gap width

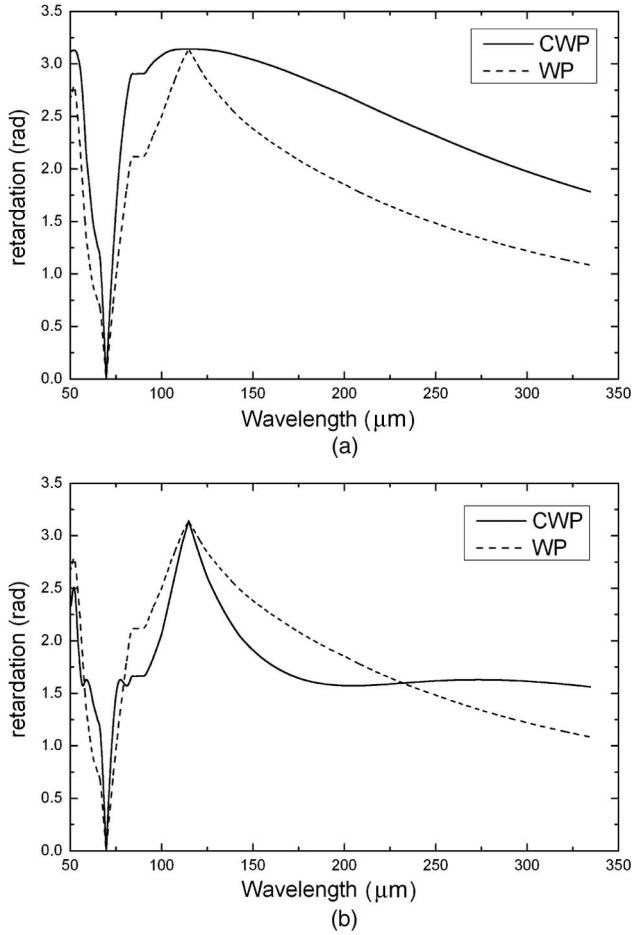

Fig. 2. (a) Comparison of the retardation of the TWPC in half-wave mode, 120 μm wavelength, with the monochromatic WP for the same wavelength. (b) Comparison of the retardation of the TWPC in quarter-wave mode, 230 μm wavelength, with the monochromatic WP for the same wavelength.

(about some micrometers). In the case of a wedge-shaped gap the calculation taking into account the interference is possible, but one should know the wedge width. This is unlikely in practice. In this case one should integrate with the small areas of the plate, each area being related to the concrete gap width in the given point. In this work, the authors experimentally show that there is no need to take the interference effect into account.

Use of the matrix 4×4, described in [10], instead of Eq. (1) is feasible when the interference must be taken into account due to practical considerations, for example, when the spectral bandwidth of the source is less than the typical width of the diffraction maxima. Wavelength bandwidth can be estimated from a simple formula, $\Delta\lambda = \lambda^2 \Delta f / c$, where Δf is the frequency bandwidth. It should be compared to the interference period obtained from the $\delta(\lambda)$ curve for the same wavelength. Whenever $\Delta\lambda$ exceeds the interference period, the matrix (1) is generally sufficient for use. It should be noted that in the case of the monochromatic WP the interference effect is also present.

Examples of the theoretical dependence of the retardations $\delta(\lambda)$, calculated for the cases of 2×2 and 4×4 Jones matrices, are shown in Fig. 3 (the cases of half-wave and quarter-wave plates). It can be seen that the general shapes of the curves for different Jones matrices are the same, but the interference effect leads to "noisiness" of the curves at specific wavelengths.

B. Experimental Results

1. *TWPC*

Experimental approval of the method has been carried out with the use of the Fourier spectrometer Vertex 70, with the measurements in transmission mode. During the experiment the system of three parallel quartz plates was situated in the spectrometer. We have rotated each plate individually with the use of axial rotation mounts. The system of the plates was situated between two linear polarizers. The first one, situated on the THz beam source aperture, was fixed. The second one, situated after the plate set, was rotatable. The angular position for each plate was calculated according to the mathematics described in Section 2.A. The relation with transmission and retardation occurred through the Jones matrix and was described in detail in [14]. The transmission spectra were normalized to the value of the transmission of two polarizers with the polarization axes parallel to each other.

Figure 4 depicts the theoretical and experimental transmission spectra of the TWPC situated between two parallel linear polarizers. The theoretical transmission was calculated with the multiplication of the Jones matrix of the system on the polarizer matrices. The TWPC is in half-wave mode for 120 [Fig. 4(a)] and 250 [Fig. 4(b)] μm wavelengths. It can be seen that in 105–130 μm [Fig. 4(a)] and 230–270 μm [Fig. 4(b)] wavelength ranges the transmission is

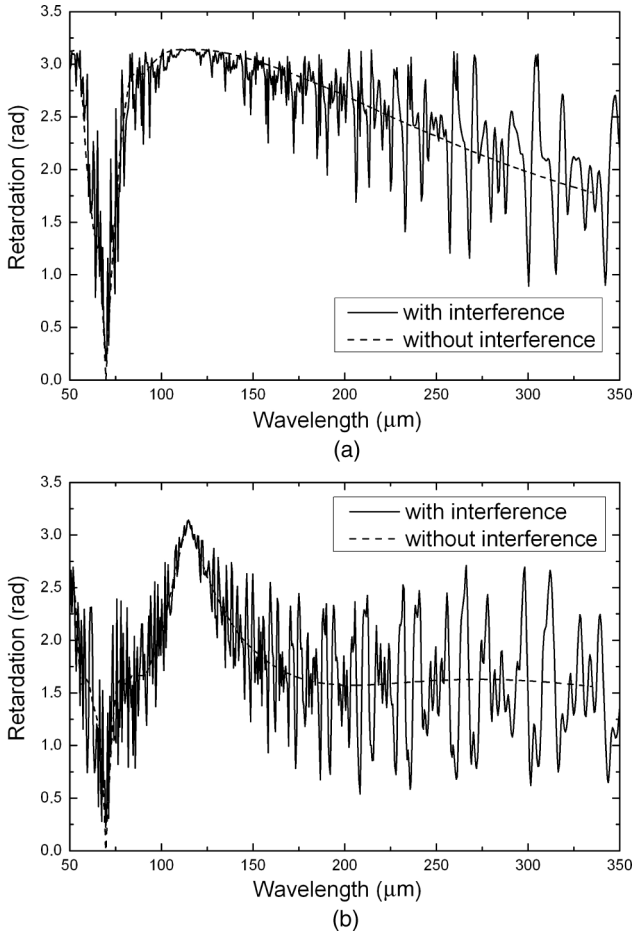

Fig. 3. (a) Comparison of the retardation with and without the effect of the interference of the TWPC in half-wave mode, 115 μm wavelength. (b) Comparison of the retardation with and without the effect of the interference of the TWPC in quarter-wave mode, 250 μm wavelength.

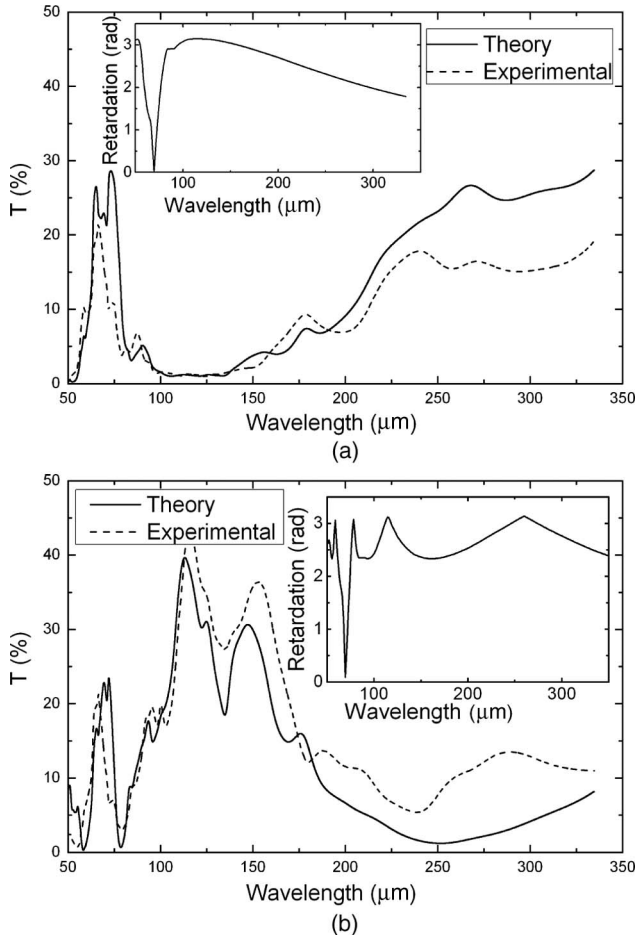

Fig. 4. Theoretical and experimental transmission spectra of the TWPC in half-wave mode situated between two parallel linear polarizers: for (a) 120 and (b) 250 μm wavelengths. Insets: dependence of the retardation on the wavelength.

close to zero; therefore the TWPC really works as a half-wave waveplate. The deviation from zero of the experimental curve in Fig. 4(b) is associated with low SNR of Fourier spectrometer in this wavelength range. The dependence of the retardation on the wavelength is shown in the insets. Here one can see that for the pointed wavelength the value of the retardation is π.

In Fig. 5 the theoretical (a) and experimental (b) transmission spectra of the TWPC situated between two linear polarizers are shown. The TWPC is in quarter-wave mode for 220 μm wavelength. Each spectrum in the set is related to the special angle of the polarization axis of the second polarizer (analyzer): in this case, we have −32, 13, and 58 deg. It is seen that the transmission of this system does not depend on this angle; i.e., linearly polarized light is being transformed effectively into the circularly polarized light for the specified wavelength. This means that the TWPC works similarly to the quarter-wave monochromatic WP at this wavelength. The small misfit of the curves is related to relatively low SNR of the spectrometer in the wavelength range being discussed. The dependence of the retardation on the wavelength is shown in the inset. Here one can see that for the pointed wavelength the value of the retardation is $\pi/2$.

Additionally, in Fig. 6, the dependence of the transmission on the angular position of the analyzer for linear [Fig. 6(a)] and circular [Fig. 6(b)] polarizations is shown. It is clearly seen that this dependence has known $\cos^2(\varphi)$ and almost perfect circular character, respectively.

It should be noted that the wavelength range of TWPC possible adjustment depends on the thickness of the plates (and, of course, on the retardation accuracy), and, with the use of three to four different sets, may cover the whole THz region. Also it should be noted that the TWPC allows the transformation of the polarization in general, i.e., not only linear to circular and circular to linear, but also elliptic to elliptic (with the given axis ratio and angle between the axes of the input and output light).

All the experimental results discussed in this section show that the agreement of the theory with the experiment is very good. All the experiments are in agreement with the theoretical model proposed on the basis of the TWPC calculation, which allows the authors to use the results in practice—in the

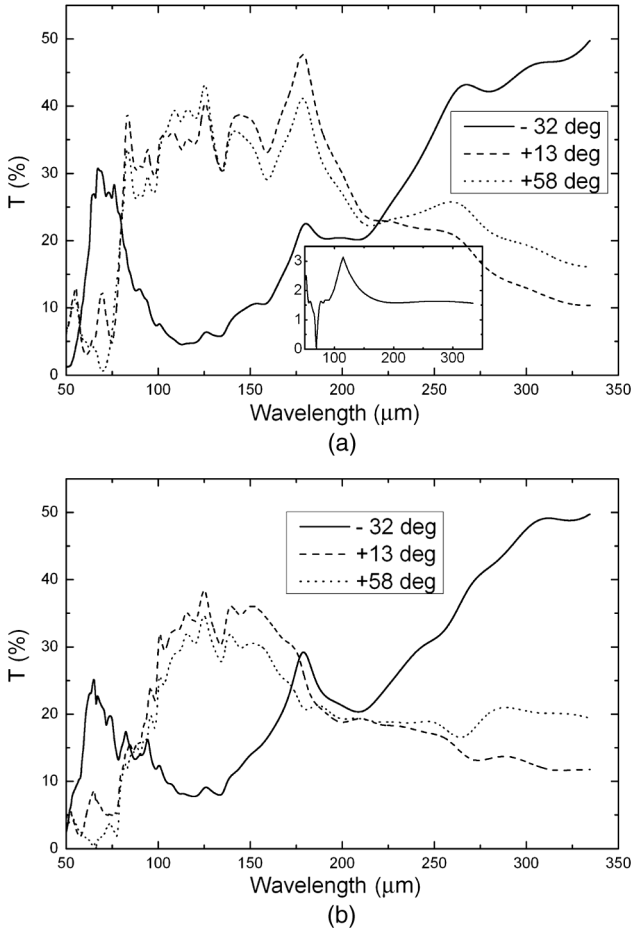

Fig. 5. (a) Theoretical and (b) experimental dependence of linearly polarized light transmission for $\lambda/4$ TWPC on 220 μm wavelength for different angles of analyzer (rotated linear polarizer: −32, 13, and 58 deg). Inset: dependence of the retardation (radians) on the wavelength (micrometers).

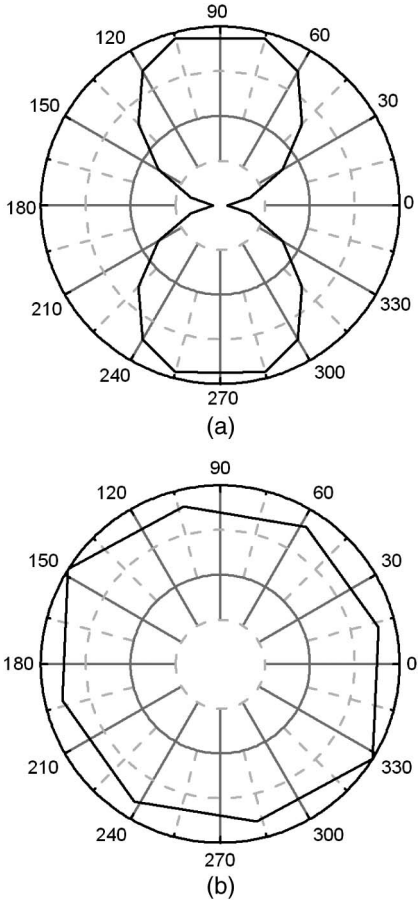

Fig. 6. Dependence of the transmission on the angular position of the analyzer for (a) linear and (b) circular polarizations. (a) Case of linear-to-linear (rotated to 90 deg) polarization transformation at 120 μm wavelength. (b) Case of linear-to-circular polarization transformation at 200 μm wavelength.

experiments in which the transformation of the light polarization is necessary.

2. *Solc Band Pass Filter and Achromatic Waveplate*

Our experiments show that the TWPC may be used as a Solc filter [15] if the angular positions of the plates are appropriately chosen. The angles in our case are +15, −15, and +15 deg (which is related to a crossed Solc filter); they were calculated according to theory [15,17]. There is no possibility to tune the transmission band of this filter, because it depends on the plate thickness. To work in this mode one should situate the TWPC between crossed linear polarizers. In Fig. 7 the theoretical and experimental transmission spectra of this system are shown. The system represents a Solc filter at 125 μm wavelength. The experiment is in good agreement with the theory. The small misfit of the curves is related to relatively low SNR of spectrometer in the wavelength range being discussed.

Also the TWPC may be used as an achromatic waveplate (AWP) in the small wavelength range. The theory of the AWP calculation is described in [9,10,14]. For example, Fig. 8 shows the comparison of the theoretical and experimental transmission of the TWPC tuned in AWP mode. It can be seen that in the 60–180 μm wavelength range this system may

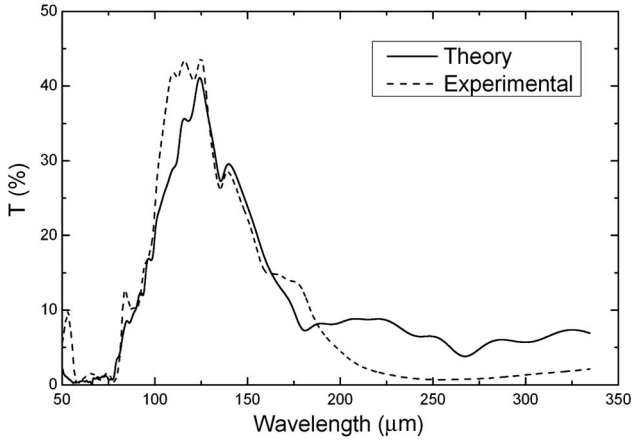

Fig. 7. Theoretical and experimental transmission spectra of the TWPC tuned in Solc filter mode at 125 μm wavelength.

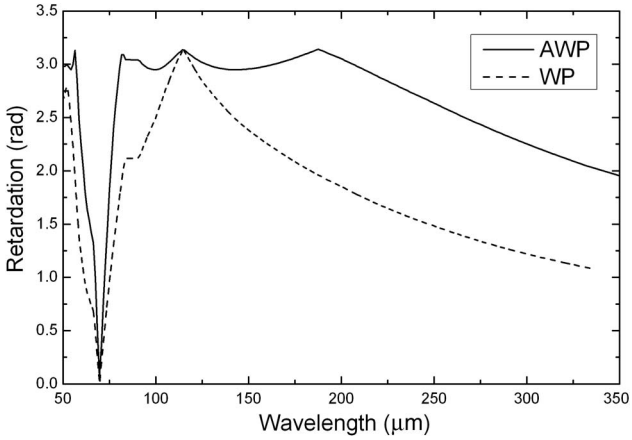

Fig. 8. Comparison of the theoretical and experimental transmission of the TWPC tuned in AWP mode.

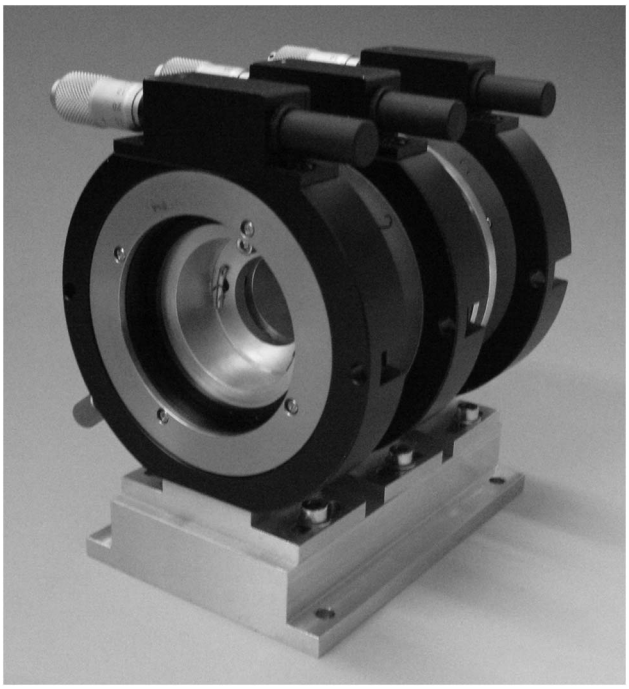

Fig. 9. Tunable wavelength polarization converter.

be used as a half-wave AWP with retardation accuracy about ±5%.

In general, in this paper the authors experimentally show that tuning of the TWPC in different working modes is possible. First, it is possible to use the TWPC as a quarter-wave plate in the arbitrary wavelength range (in our case it was 160–270 μm), and as a half-wave plate also in the arbitrary wavelength range (in our case 80–180 μm). Second, the authors have used the TWPC as a Solc band pass filter (in our case at 125 μm). Third, the possibility to use the TWPC as an AWP (in our case it was 60–180 μm) was also demonstrated.

3. Conclusion

We have demonstrated by experiments that sets of plane-parallel birefringent plates with in-plane birefringence axes are instrumental for THz polarization optics. We present results of calculations and experimental validation of the tunable wavelength polarization converter for the THz spectral range for different (arbitrary) retardations (π and $\pi/2$ in our case). The possibility to use the TWPC as a Solc band pass filter and AWP was demonstrated. Good agreement with Jones formalism was shown in all cases. Also, an experimental device (see Fig. 9) was produced and tested.

This work was supported by the Russian Foundation for Assistance to Small Innovative Enterprises (FASIE), contract No. 12234p/23287.

References

1. J. Federici, B. Schulkin, F. Huang, D. Gary, R. Barat, F. Oliveira, and D. Zimdars, "THz imaging and sensing for security applications—explosives, weapons and drugs," Semicond. Sci. Technol. **20**, S266–S280 (2005).
2. F. Friederich, W. von Spiegel, M. Bauer, F. Meng, M. Thomson, S. Boppel, A. Lisauskas, B. Hils, V. Krozer, A. Keil, T. Loffler, R. Henneberger, A. Huhn, G. Spickermann, P. Bolivar, and H. Roskos, "THz active imaging system with real-time capabilities," IEEE Trans. Terahertz Sci. Technol. **1**, 183–200 (2011).
3. K. Ajito and Y. Ueno, "THz chemical imaging for biological applications," IEEE Trans. Terahertz Sci. Technol. **1**, 293–300 (2011).
4. K. Humphreys, J. Loughran, W. Lanigan, T. Ward, J. Murphy, and C. O'Sullivan, "Medical applications of terahertz imaging: a review of current technology and potential applications in biomedical engineering," in *Proceedings of IEEE 26th Annual International Conference of the Engineering in Medicine and Biology Society* (IEEE, 2004), pp. 1302–1305.
5. X.-C. Zhang and J. Xu, *Introduction to THz Wave Photonics* (Springer, 2010).
6. Z. Taylor, R. Singh, D. Bennett, P. Tewari, N. Bajwa, M. Culjat, A. Stojadinovic, H. Lee, J.-P. Hubschman, E. Brown, and W. Grundfest, "THz medical imaging: in vivo hydration sensing," IEEE Trans. Terahertz Sci. Technol. **1**, 201–219 (2011).
7. F. Brehat and B. Wyncke, "Measurement of the optical constants of crystal quartz at 10 K and 300 K in the far infrared spectral range: 10–600 cm^{-1}," J. Infrared Millim. Terahertz Waves **18**, 1663–1679 (1997).
8. M. Darsht, "The influence of an external factors on the polarized light propagation," Ph.D. thesis (Chelyabinsk, 1996) (in Russian).
9. J.-B. Masson and G. Gallot, "Terahertz achromatic quarter-wave plate," Opt. Lett. **31**, 265–267 (2006).
10. G. Savini, G. Pisano, and P. Ade, "Achromatic half-wave plate for submillimeter instruments in cosmic microwave background astronomy: modeling and simulation," Appl. Opt. **45**, 8907–8915 (2006).
11. S. Pancharatnam, "Achromatic combination of birefringent plates," Proc. Ind. Acad. Sci. A **XLI**, 130–144 (1955).
12. J. Ma, J.-S. Wang, C. Denker, and H.-M. Wang, "Optical design of multilayer achromatic waveplate by simulated annealing algorithm," Chin. J. Astron. Astrophys. **8**, 349–361 (2008).
13. G. Kang, Q. Tan, X. Wang, and G. Jin, "Achromatic phase retarder applied to MWIR & LWIR dual-band," Opt. Express **18**, 1695–1703 (2010).
14. A. K. Kaveev, G. I. Kropotov, E. V. Tsygankova, I. A. Tzibizov, S. D. Ganichev, S. N. Danilov, P. Olbrich, C. Zoth, E. G. Kaveeva, A. I. Zhdanov, A. A. Ivanov, R. Z. Deyanov, and B. Redlich, "Terahertz polarization conversion with quartz waveplate sets," Appl. Opt. **52**, B60–B69 (2013).
15. A. Yariv and P. Yeh, *Optical Waves in Crystals* (Wiley, 1987).
16. R. Jones, "A new calculus for the treatment of optical systems," J. Opt. Soc. Am. **31**, 488–503 (1941).
17. A. Ghosh and A. Chakraborty, "A mixed Solc birefringent filter," Opt. Acta **29**, 1407–1412 (1982).